Coulomb impurity effect on Dirac electron in graphene magnetic dot

Lee, C. M.; Chan, K. S.

Published in:
Journal of Applied Physics

Published: 14/10/2013

Document Version:
Final Published version, also known as Publisher's PDF, Publisher's Final version or Version of Record

Published version (DOI):
10.1063/1.4824808

Publication details:
Lee, C. M., & Chan, K. S. (2013). Coulomb impurity effect on Dirac electron in graphene magnetic dot. *Journal of Applied Physics*, *114*(14), Article 143708. https://doi.org/10.1063/1.4824808

Coulomb impurity effect on Dirac electron in graphene magnetic dot

Cite as: J. Appl. Phys. **114**, 143708 (2013); https://doi.org/10.1063/1.4824808
Submitted: 12 August 2013 • Accepted: 25 September 2013 • Published Online: 11 October 2013

C. M. Lee and K. S. Chan

JOURNAL OF APPLIED PHYSICS **114**, 143708 (2013)

Coulomb impurity effect on Dirac electron in graphene magnetic dot

C. M. Lee[1,a)] and K. S. Chan[1,2,b)]
[1]*Department of Physics and Materials Science and Center for Functional Photonics, City University of Hong Kong, Tat Chee Avenue, Kowloon, Hong Kong, People's Republic of China*
[2]*City University of Hong Kong, Shenzhen Research Institute, Shenzhen, People's Republic of China*

(Received 12 August 2013; accepted 25 September 2013; published online 11 October 2013)

Using the Dirac-Weyl model, we study the low-lying spectra of a massless Dirac electron bound to a positively charged Coulomb impurity in a graphene magnetic dot, for which the inhomogeneous magnetic field is created by different magnetic fields inside and outside the dot with a field ratio α. Numerical results show that the zero energy states, in the presence of the impurity, are converted into hole-like states. Additionally, for positive and negative α values, the states are, in general, located inside and outside the dot, respectively, causing the spectra to exhibit different features. © *2013 AIP Publishing LLC*. [http://dx.doi.org/10.1063/1.4824808]

I. INTRODUCTION

In the past decade, the magnetic dot was a subject of intense theoretical and experimental interest[1–9] since the isolation of monolayer and few-layer graphene sheets by Novoselov *et al.*[10,11] Owing to the exceptionally high carrier mobility and long spin relaxation time at ambient environment, graphene is now considered as a promising candidate for high density memory devices or spintronic materials.

The energy band structure of graphene is unique. The energy-momentum (E-k) dispersion at low energies is linear near the K and K' valleys in the Brillouin zone. The charged particles in graphene can then well be described as massless relativistic fermions and are governed by the Dirac-Weyl (DW) model rather than the nonrelativistic Schrodinger model. In perpendicular homogeneous magnetic fields (B), the relativistic Landau energy levels for such a massless Dirac electron is given by $E \propto \pm\sqrt{BN}$, while the nonrelativistic one for a massive Schrodinger electron is given by $E \propto BN$, where N is the Landau level (LL) index.

The charged Dirac electrons in graphene, owing to the Klein effect,[12] cannot be confined by electrostatic barrier. Some theoretical attempts have been proposed to trap the particles and to form quasi-bound states by using electrostatic potentials.[13–16] Another alternative approach is to confine by magnetic barriers. On the theoretical side, magnetic dots are examples to have a good start since in general highly symmetrical mathematical models can be easily constructed. For monolayer graphene, Martino *et al.* earlier gave an interesting proposal to confine electrons by inhomogeneous magnetic fields.[1–4] Various inhomogeneous magnetic field configurations were then considered including exponentially decaying fields,[5] non-zero fields in a circular dot,[6] fields corresponding to various potentials,[7] circular step fields,[8,9] different fields between domains,[17] and even δ-function magnetic barriers.[18] In all these studies, discontinuous and/or inhomogeneous magnetic fields were considered to find out the field dependences of the low-lying spectra and the energy dependences of the transmission probability through the magnetic barriers, and the electron states, including bound, quasi-bound, and scattering states. They all conclude that electrons can be confined by magnetic barriers in monolayer graphene. In experiments, magnetic dots are realized effectively by creating inhomogeneous magnetic fields in the systems.[19] Deposition of ferromagnetic or superconducting material on graphene substrate, and strain induced pseudo-magnetic fields are some of the examples considered.

The properties of such magnetic dot systems including impurities are one of the interests in this area since they modify the energy levels of the materials and in turn affect their electronic and optical properties. However, studies of those above-mentioned magnetic field configurations with impurities involved[20–22] in more realistic experimental situations are rare. In the present article, we study the DW model for a graphene magnetic dot system,[6] bound to an on-center positively charged Coulomb impurity, in which the magnetic fields inside and outside the dot are different constant values with a ratio α. This field profile can be realized by placing the ferromagnetic circular disk on top of the graphene layer. We use numerical diagonalization to calculate the low-lying spectra, as a function of α, including positive energy, negative energy, and zero-energy states, and also their binding energies due to the Coulomb potential. Finally, we compare and analyze our overall results for such a system with and without an impurity.

II. THEORY

For low-energy approximation, the massless DW Hamiltonian in graphene close to the K and K' valleys describing a single electron in a magnetic dot with an on-center positively charged Coulomb impurity reads[20–22]

$$\hat{H} = v_F \sigma \cdot (\mathbf{P} + e\mathbf{A}) + V_{\text{coul}}\mathbb{I}, \tag{1}$$

where v_F is the electron's Fermi velocity, with the value of about 1/300 of photon's, instead of the photon's in conventional DW equation. $\sigma = (\sigma_x, \sigma_y)$ and $\mathbb{I}$ are the 2×2 Pauli matrices in the pseudospin space, and the identity matrix, respectively. $\mathbf{P}$ and $\mathbf{A}$ are the momentum operator and the

a)Electronic mail: mesimon_hk@yahoo.com.hk
b)Electronic mail: apkschan@cityu.edu.hk

vector potential in the two-dimensional (2D) space, respectively. The Coulomb potential between the electron and the on-center impurity is in the two diagonal matrix elements of the DW Hamiltonian, i.e., the last term of Eq. (1), which is given by

$$V_{\text{coul}} = -\frac{e^2}{4\pi\epsilon r}, \tag{2}$$

where the minus sign indicates the Coulomb interaction between the electron and the impurity is attractive. Note that K-K' mixing is neglected in Eq. (1).[1,20,23] In the present case, the magnetic dot is created by the following inhomogeneous magnetic fields: the magnetic fields inside and outside the dot region are constant but with different values, and both are perpendicular to the dot xy-plane, i.e., the inner magnetic field $B(r) = \alpha B_0$ for $0 \le r < r_0$, while the outer magnetic field is B_0 for $r \ge r_0$. The directions of the inner and outer magnetic field are opposite when the field ratio α is negative. The field is uniform over the whole system for $\alpha = 1$, while the field is zero inside the dot for $\alpha = 0$. The corresponding vector potential A with circular symmetry can be derived by using the relationship between the magnetic flux $\Phi(r)[= 2\pi r A(r)]$ and the enclosed area integral of $B(r)$, which can be represented in the polar coordinates as

$$A(r) = \begin{cases} \dfrac{\alpha B_0 r}{2} & \text{for } 0 \le r < r_0, \\ \dfrac{B_0(r^2 - (1-\alpha)r_0^2)}{2r} & \text{for } r \ge r_0. \end{cases} \tag{3}$$

In order to obtain the numerical solution for the original Hamiltonian by direct diagonalization, the DW Hamiltonian is simplified and separated into two parts, the unperturbed term $\hat{H}_0$

$$\hat{H}_0 = v_F \begin{pmatrix} 0 & \hat{\pi}_0^- \\ \hat{\pi}_0^+ & 0 \end{pmatrix} \tag{4}$$

with

$$\hat{\pi}_0^{\pm} = \pm j \exp(\pm j\theta)\left[\mp\hbar\frac{\partial}{\partial r} + \frac{l\hbar}{r} + \frac{erB_0}{2}\right], \tag{5}$$

and the residual potential term

$$\hat{V} = \begin{pmatrix} \hat{V}_{\text{coul}} & \hat{V}_+ \\ \hat{V}_- & \hat{V}_{\text{coul}} \end{pmatrix}. \tag{6}$$

The two-component spinor, as the bases for numerical diagonalization, with each component corresponding to a sublattice of graphene, is written as

$$\Psi_{nl}^T = (\,\phi_{N-1,l-1} \quad j\phi_{N,l}\,), \tag{7}$$

where $\phi_{N,l}$ can be chosen as the well-known 2D harmonic product basis states, with nonnegative integer LL index $N[\equiv n + (l + |l|)/2]$. n and $l\hbar$ are the radial quantum number and the orbital angular momentum, respectively. The phase factor $\exp(\pm j\theta)$ for both off-diagonal matrix elements in $\hat{H}_0$ and also in $\hat{V}$, as given later, can be canceled out after integration, since the angular momenta of the two spinor components are differed by one unit. The two operators in $\hat{H}_0$ are regarded as raising and lowering operators. Therefore, the corresponding eigenvalue for the $\hat{H}_0$ is obtained by $E_{N,l} = \pm N^{\frac{1}{2}}$ in energy unit of $\hbar\omega(\equiv \sqrt{2}v_F\hbar/a)$ with the magnetic length $a(\equiv \sqrt{\hbar/eB_0})$. The $\pm$ sign represents the electron-hole symmetry. Note that, although the quantum states of the two spinor components are different, see Eq. (7), for easy comparison, we use the same notations for the quantum states of those electron-hole pairs in all the figures without affecting our analysis, according to their LL indices, N.

In Eq. (6), the matrix elements of the residual potential are rewritten in dimensionless unit, after simplification, as

$$\hat{V}_{\text{coul}} = \frac{C}{r}, \tag{8}$$

$$\hat{V}_{\pm} = \mp j \exp(\mp j\theta) \times \frac{-1}{2\sqrt{2r}} \times \begin{cases} (1-\alpha)r^2 & \text{for } 0 \le r < r_0, \\ (1-\alpha)r_0^2 & \text{for } r \ge r_0, \end{cases} \tag{9}$$

and, in the diagonal terms [Eq. (8)], the Coulomb parameter C represents the interaction strength of the electron with the on-center impurity, and is given by

$$C = \frac{e^2}{2\sqrt{2}\epsilon v_F h}, \tag{10}$$

which is measured in unit of magnetic length, while the nondiagonal terms in Eq. (9) are associated with the missing magnetic flux in the magnetic dot system. In our present numerical calculation, 30 pairs of lowest basis states for a particular angular momentum l is used for numerical diagonalization.

III. DISCUSSION AND CONCLUSIONS

Based on the above formalism, we set the magnetic dot to be of two different sizes, $2a$ and $4a$, and make numerical calculation for their low-lying spectra as a function of the field ratio α, i.e., the inner magnetic field is varying, while the outer one keeps constant. The quantum states are limited to $n \le 2$ and $|l| \le 3$. And the Coulomb parameter is set to be $C = 0.5$. The inner and the outer magnetic fields hereafter for simple notation are denoted by B_{in} and $B_{\text{out}}(= B_0)$, respectively. In all figures, the states are labeled by $(n, l)^{\pm}$, for which the superscripts "$\pm$" represent the positive (or electron) and the negative (or hole) energy states, respectively, while the original highly degenerate zero energy states as exceptions are denoted by the superscript "0".

Using the impurity-free cases as references, we plot their low-lying spectra as a function of α for different dot sizes, $r_0 = 2a$ and $4a$ in Figs. 1(a) and 2(a), respectively. From the figures, we see that both the spectra show the electron-hole symmetrical structure about the horizontal axis. The zero energy states remain highly degenerate lying at zero energy as α changes from 1. And the upper part is the

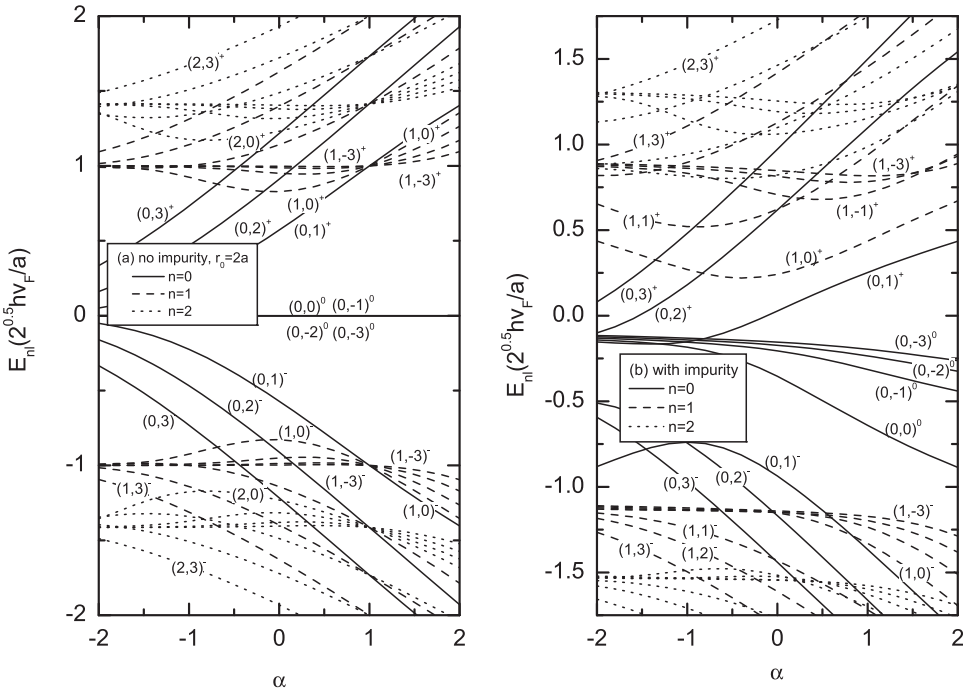

FIG. 1. Low lying spectra of a magnetic dot with a dot size $r_0 = 2a$ as a function of the field ratio α (a) without impurity and (b) with an impurity.

positive energy (or electron) states, while the lower one is the negative energy (or hole) states. Owing to the electron-hole symmetry, we discuss the spectra only for the positive energy states. The figures show that the angular momentum states are highly degenerate lying at all the corresponding bulk LLs ($N > 0$) for $\alpha = 1$, since the whole system is in a uniform magnetic field. The spectra exhibit different features for different dot sizes as α increases and decreases from 1. Here, we focus on the (n, $l \leq 0$) states. In Fig. 1(a), for a small dot size ($r_0 = 2a$), the corresponding bulk LLs are nondegenerate and split into discrete angular momentum states with the reverse level ordering at $\alpha = 1$. When B_{in} for $\alpha > 1$ is stronger, the (n, $l \leq 0$) states are pushed toward the dot center and the electron moves in a uniform field B_{in}. Their eigenenergies will increase appreciably since the eigenvalues for their corresponding LL is proportional to $\sqrt{B_{\text{in}}}$ or $\sqrt{\alpha}$. Besides, the higher the $|l|$ at a given LL, the further the state is away from the dot center, and locates much nearer to or even outside the edge of the dot, leading its eigenenergy to deviate downward much further away from the corresponding bulk LL. This can be seen from Fig. 1(a) that the state (1,0), as the closest to the dot center, deviates the least from the bulk LL as compared with the neighboring ones for the first LL ($N = 1$) as an example. For a larger dot size ($r_0 = 4a$), in Fig. 2(a), since all angular momentum states, including (n, $l > 0$), for given LLs are far away from

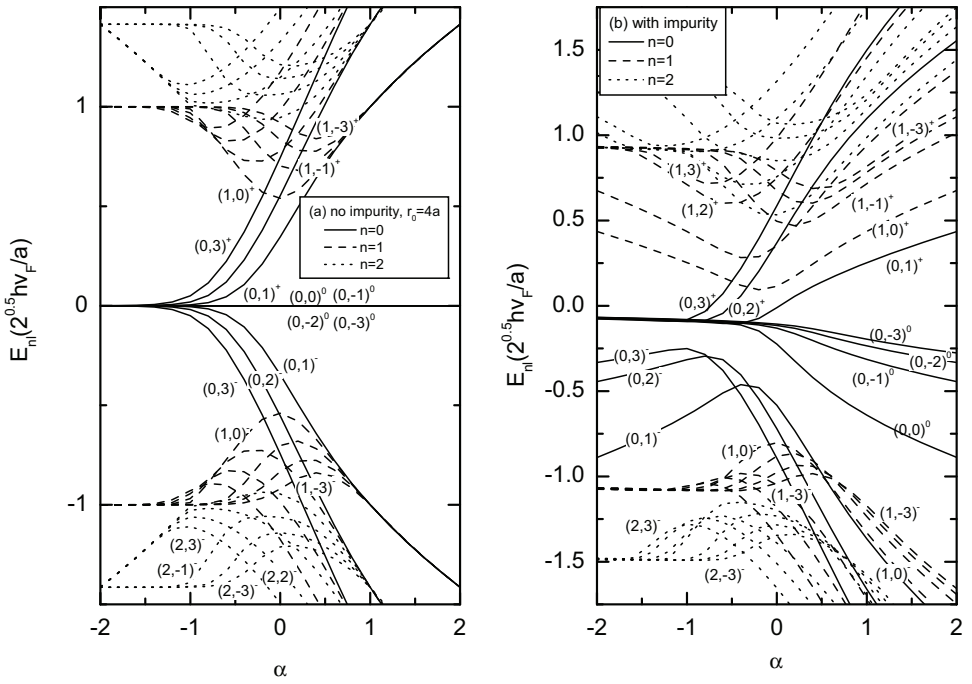

FIG. 2. The same as Fig. 1 for a magnetic dot with a larger dot size, $r_0 = 4a$.

the dot edge and much closer deep around the dot center. The electron moves in uniform inner magnetic fields. All the states are highly degenerate lying at their corresponding bulk LLs, and their eigenenergies increase monotonically with $\sqrt{\alpha}$.

Conversely, when α decreases to zero from 1, we see from the small and large dot sizes in Figs. 1(a) and 1(b), respectively that B_{in} will become weaker and cause the states further away from the dot center and even from the dot edge. When its value changes further from zero to negative, the states are now repelled by B_{in} to be much further away from the dot edge and the electron will move in a uniform outer magnetic field B_{out} finally. Its eigenenergies approach to their constant values for corresponding LLs induced by a constant B_{out}, being independent of α. Among the states, take the first LL as an example, the state (1,-3) is the farthest from the dot edge and the effect of inhomogeneous magnetic field at the dot edge is the least. This state is therefore the nearest to the bulk LL within a very large range of α, even up in a uniform magnetic field over the whole system, i.e., $\alpha = 1$.

For those positive angular momentum states, three notes are required to be made here that, (a) $(n, l > 0)$ states move in a magnetic field is equivalent to the $(n, -l)$ states in a magnetic field with opposite direction, (b) and therefore, when α decreases down to -2, we see for the large dot size ($r_0 = 4a$) in Fig. 2(a) that those states (0,1),(0,2),(0,3) all merge to the zero LL outside the dot although they approach to different LLs inside the dot for large positive α value, while (c) for the small dot size ($r_0 = 2a$) in Fig. 1(a), those positive angular momentum states remain nondegenerate, although the dot size is very small, and sufficiently large negative α value will be required to make them merge to their corresponding bulk LLs. In other words, the smaller the dot size, the smaller the effect of the inverse B_{in} on the angular momentum states and larger inverse B_{in} will be required to merge them into the degenerate states.

Let us now consider the case with an on-center positively charged impurity. The corresponding low-lying spectra for small and large dot sizes are plotted in Figs. 1(b) and 2(b), respectively. We see from the figures that the whole spectra shift downward and the electron-hole symmetrical structure are broken apparently. The originally highly degenerate zero energy states start to be nondegenerate and split into discrete angular momentum states at certain α. Since the Coulomb potential of the positively charged impurity attracts the electron, the zero-energy states are now converted into hole-like states. Among these states, $(0, -3)^0$ is the nearest one to the zero energy, and is the most stable, since it is the farthest from the dot center and its interaction with the positively charged impurity is the least. While for negative α values, these states including those positive angular momentum states, i.e., $(0, 1)^+$, $(0, 2)^+$, $(0, 3)^+$, merge to a degenerate state with the eigenenergy lowered by a definite amount as compared with those of impurity-free case. This implies the Coulomb effect still remains significant although the electron is much further away from the dot.

For the large dot size [Fig. 2(b)], in the negative energy states, there exists a critical point of reverse level ordering at a positive α value for each LL. Above the critical α, the level ordering is similar to that of the zero energy states. This implies the Coulomb effect is still significant. Below the critical point, the level ordering returns to those of the impurity-free case and the magnetic confinement becomes dominant. For negative α, the states including $(n \geq 1, l > 0)^-$ merge to corresponding degenerate eigenenergies with downward shifts by definite amounts, as compared with their bulk LLs, due to the Coulomb potential, with the states $(0, l > 0)^-$ as exceptions. For these exceptional states, their eigenenergies show apparent increase with $|\alpha|$ implying that they are much closer to the dot center, and thus mostly affected by B_{in} rather than B_{out}. This fact can also be clarified by their very large binding energy at large negative α due to Coulomb potential, see $(0, 1)^-$ in Fig. 3, as discussed later. In the positive energy states, reverse level ordering with critical points similar to those of negative energy states cannot be observed, since the Coulomb potential and the magnetic confinement have the similar effects on the electron states. Instead, the positive energy states for a given LL increase separately for positive α values.

Fig. 1(b) shows that the spectra of the small dot size ($r_0 = 2a$) are qualitatively similar to those of the large one ($r_0 = 4a$). Nevertheless, there are some differences that, (a) even in the positive energy states, there exists a point of reverse level ordering at the first LL (N = 1), (b) in the negative states, there is no point of the reverse level ordering at the first LL (N = 1), and these highly degenerate states start

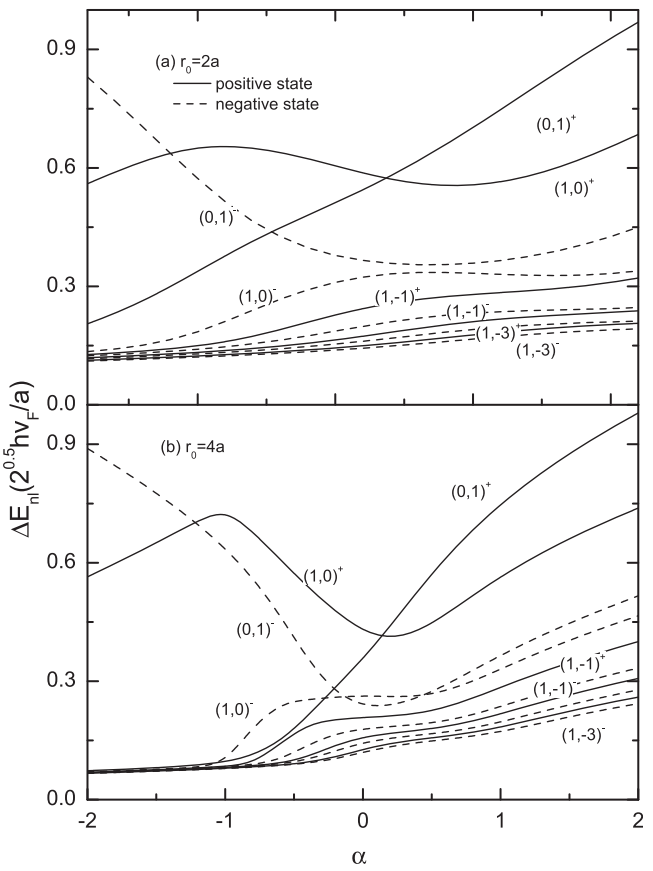

FIG. 3. Corresponding binding energy for the quantum states of the first LL of the magnetic dot considered in Figs. 1 and 2.

to be nondegenerate at $\alpha \approx 0.5$ instead, since the Coulomb effect is much significant compared with the magnetic confinement.

In order to further study the effect of the impurity on the spectra, we define the binding energy $\Delta E_{(n,l)^{\pm}}$ as the difference between the eigenenergies with and without the Coulomb potential. As to be known that the Coulomb potential is proportional to $1/r$, therefore it can be used as an indicator of the change of the electron position. Using those energy states of the first LL ($N=1$) for both dot sizes in Figs. 1 and 2 as examples, we plot the corresponding binding energies as functions of α in Fig. 3. The figures, for negative angular momentum states, show that the binding energies increase monotonically as α increases from negative to positive. This well agrees with those discussed previously that the states approach nearer to the dot center as α increases, and the Coulomb potential increases subsequently. For a given angular momentum state, the positive energy states have higher binding energies than the negative ones. Furthermore, the lower angular momentum states $|l|$ are much closer to the impurity at the dot center and have higher binding energies as compared with the neigboring ones. As to be known that the average orbit for the electron moving around the center at a certain magnetic field is given by the mean square orbit radius, $\langle r^2 \rangle \propto 2n + |l| + 1$. Among the first LL, the orbit size of the angular momentum states (0,1) and (1,0) are the most nearest to the dot center. They have extremely high binding energies even in negative α, since they are pushed deep very near to the dot center by the inner magnetic field, which is confined much deep inside the dot. Also local maximum and minimum are present in the binding energies because of the competition between the Coulomb potential and the magnetic confinement.

Finally, when we compare the entire low-lying spectra of the magnetic dot in the present work with those of the Schrodinger model,[24] we note two features: (a) in the absence of impurity and under magnetic fields, originally degenerate ground states or the lowest LL become nondegenerate in the Schrodinger model, but remain unchanged in the Dirac model, and (b) in the presence of a negatively charged impurity, the point of reverse level ordering exists even at the lowest LL for the Schrodinger model, but not at the lowest LL for the Dirac model.

In summary, using the DW model, we study the low-lying spectra of a single electron magnetic dot, bound to a positively charged Coulomb impurity, as a function of field ratio, $B_{\text{in}}/B_{\text{out}}$. There are several remarks for the numerical results of two different dot sizes.

(1) In the presence of the positively charged Coulomb impurity, the electron-hole symmetrical structure of the spectra is broken by the Coulomb potential and the zero energy states are converted into hole-like states. For higher neigboring LLs of the large dot ($r_0 = 4a$), there exist points of reverse level ordering in the negative energy states but not in the positive ones.
(2) The qualitative aspect of the spectra only depends on the field ratio α, but not on the actual strength of the magnetic field applied. For positive and negative α values, the states are in general located inside and outside the dot, respectively, causing the spectra to exhibit different features.
(3) From the above analysis, it can be expected that, when the positively charged impurity is replaced by a negatively charged one, the spectra for positive energy states and negative energy states are just reversed, and the zero energy states are converted into electron-like ones.

ACKNOWLEDGMENTS

This work was supported by the General Research Fund of the Research Grants Council of Hong Kong SAR, China, under Project No. CityU 100311/11 and National Natural Science Foundation of China. (NSFC, Grant No. 11274260).

[1]A. D. Martino, L. Dell' Anna, and R. Egger, Phys. Rev. Lett. **98**, 066802 (2007).
[2]A. D. Martino, Solid State Commun. **144**, 547 (2007).
[3]L. Dell'Anna and A. D. Martino, Phys. Rev. B **79**, 045420 (2009).
[4]A. D. Martino and R. Egger, Semicond. Sci. Technol. **25**, 034006 (2010).
[5]T. K. Ghosh, J. Phys: Condens. Matter **21**, 045505 (2009).
[6]D. Wang and G. Jin, Phys. Lett. A **373**, 4082 (2009).
[7]S. Kuru, J. M. Negro, and L. M. Nieto, J. Phys: Condens. Matter **21**, 455305 (2009).
[8]M. R. Masir, A. Matulis, and F. M. Peeters, Phys. Rev. B **79**, 155451 (2009).
[9]M. R. Masir, P. Vasilopoulos, and F. M. Peeters, J. Phys.: Condens. Matter **23**, 315301 (2011).
[10]K. S. Novoselov, A. K. Geim, S. V. Morozov, D. Jiang, Y. Zhang, S. V. Dubonos, I. V. Grigorieva, and A. A. Firsov, Science **306**, 666 (2004).
[11]K. S. Novoselov, A. K. Geim, S. V. Morozov, D. Jiang, M. I. Katsnelson, I. V. Grigorieva, S. V. Dubonos, and A. A. Firsov, Nature **438**, 197 (2005).
[12]O. Klein, Z. Phys. **53**, 157 (1929).
[13]H. Y. Chen, V. Apalkov, and T. Chakraborty, Phys. Rev. Lett. **98**, 186803 (2007).
[14]A. Matulis and F. M. Peeters, Phys. Rev. B **77**, 115423 (2008).
[15]P. Hewageegana and V. Apalkov, Phys. Rev. B **77**, 245426 (2008).
[16]Y. Song and Y. Guo, J. Appl. Phys. **109**, 104306 (2011).
[17]S. Park and H. S. Sim, Phys. Rev. B **77**, 075433 (2008).
[18]M. R. Masir, P. Vasilopoulos, A. Matulis, and F. M. Peeters, Phys. Rev. B **77**, 235443 (2008).
[19]S. J. Lee, S. Souma, G. Ihm, and K. J. Chang, Phys. Rep. **394**, 1 (2004).
[20]V. M. Pereira, J. Nilsson, and A. H. C. Neto, Phys. Rev. Lett. **99**, 166802 (2007).
[21]Y. H. Zhang, Y. Barlas, and K. Yang, Phys. Rev. B **85**, 165423 (2012).
[22]C. Liu, J. L. Zhu, and N. Yang, J. App. Phys. **113**, 224303 (2013).
[23]A. V. Shytov, M. I. Katsnelson, and L. S. Levitov, Phys. Rev. Lett. **99**, 236801 (2007).
[24]C. M. Lee, W. Y. Ruan, J. Q. Li, and R. C. H. Lee, Phys. Rev. B **71**, 195305 (2005).